Theor Chem Acc (2013) 132:1385
DOI 10.1007/s00214-013-1385-1

REGULAR ARTICLE

QM/MM study of the conversion mechanism of lysine to methylornithine catalyzed by methylornithine synthase (PylB)

Wenyou Zhu · Yongjun Liu · Rui Zhang

Received: 16 May 2013 / Accepted: 16 July 2013

Abstract Methylornithine synthase (PylB) belongs to the family of radical SAM enzymes which converts (2S)-lysine to (2R,3R)-3-methylornithine in a radical mechanism. In this paper, the mechanism of lysine mutase reaction catalyzed by PylB has been studied by using quantum mechanics/molecular mechanics approach. The calculations reveal that the PylB-catalyzed reaction follows a fragmentation–recombination mechanism involving seven elementary reaction steps. Both the hemolytic cleavage of Cα–Cβ bond of lysine and the ligation of glycyl radical with aminobutene are possible rate limiting, corresponding to the calculated energy barriers of 23.0 and 24.1 kcal/mol, respectively. The intramolecular rotation of a fragment (aminobutene) can well explain the stereochemistry of the final product. Asp 279 functions as a general acid/base, and the other pocket residues such as Asp112, Arg235, and Ser277 form a network of hydrogen bonds responsible for orientation of the substrate.

Keywords Lysine · Methylornithine · Reaction mechanism · QM/MM · Methylornithine synthase (PylB)

1 Introduction

Pyrrolysine, encoded by the natural genetic code, is the 22nd amino acid which increases the protein structure diversity [1–5]. It is necessary for the conversion of methylamines to methane in all of the known pathways [6, 7]. In the archaebacterial family *Methanosarcinaceae*, the incorporation of pyrrolysine into the three proteins (MtmB, MtbM, and MttB) in the methylamine catabolic pathway is specified by the amber stop codon UAG [8]. Pyrrolysine was firstly discovered in 2002 [2]. A series of studies has shown that five genes (pylBCDST) are both necessary and sufficient for the biosynthesis and utilization of pyrrolysine [1, 9], i.e., pylB, pylC, and pylD catalyze the biosynthesis of pyrrolysine, while pylT and pylS code for a pyrrolysine tRNA and its cognate aminoacyl tRNA synthetase [1]. Experimental evidences have confirmed that the carbon and nitrogen atoms of pyrrolysine are all derived from lysine, and a possible mechanism has been suggested, as shown in Scheme 1 [9, 10].

In this pylBCD-dependent biosynthetic pathway, methylornithine synthase (PylB) catalyzes the conversion of lysine to methyl-D-ornithine ((2R,3R)-3-methylornithine), whereas pylC and pylD catalyze the subsequent condensation and cyclization leading to pyrrolysine [9]. As the first step, the pylB-catalyzed reaction attracts much attention [10]. PylB belongs to the family of SAM-dependent (S-adenosylmethionine) radical enzymes [11, 12] and catalyzes the conversion of L-lysine to methyl-D-ornithine, in which the S chiral center of L-lysine is inverted to the R

Electronic supplementary material The online version of this article (doi:10.1007/s00214-013-1385-1) contains supplementary material, which is available to authorized users.

W. Zhu · Y. Liu (✉)
Key Lab of Colloid and Interface Chemistry, Ministry of Education, School of Chemistry and Chemical Engineering, Shandong University, Jinan 250100, Shandong, China
e-mail: yongjunliu_1@sdu.edu.cn

Y. Liu
Northwest Institute of Plateau Biology, Chinese Academy of Sciences, Xining 810001, Qinghai, China

R. Zhang
School of Agriculture, Ludong University, Yantai 264025, Shandong, China

Published online: 26 July 2013

chiral center of (2R,3R)-3-methylornithine [10]. On the basis of the crystal structure of methylornithine synthase (PylB) in complex with methylornithine and the modeled structure of lysine inside the PylB cavity, Quitterer et al. suggested a fragmentation–recombination mechanism of lysine mutase reaction [8–10, 13–16]. It is the first proposed mechanism of mutase reaction for a SAM-dependent radical enzyme to catalyze the rearrangement of carbon backbone (Scheme 2) [8, 9]. To initiate the reaction, the C–S bond of SAM is firstly broken and simultaneously an electron transfers from the $[4Fe–4S]^{+}$ cluster to the sulfonium motif of SAM, producing the Ado (5′-deoxyadenosyl) radical, as shown in Fig. 1 [11, 17–19]. Subsequently, Ado radical abstracts a hydrogen atom from Cγ methylene group of lysine. After the fragmentation and rearrangement of lysine-derived radicals, the hydrogen atom is transferred back from Ado to the substrate to complete the catalytic reaction of pylB [16].

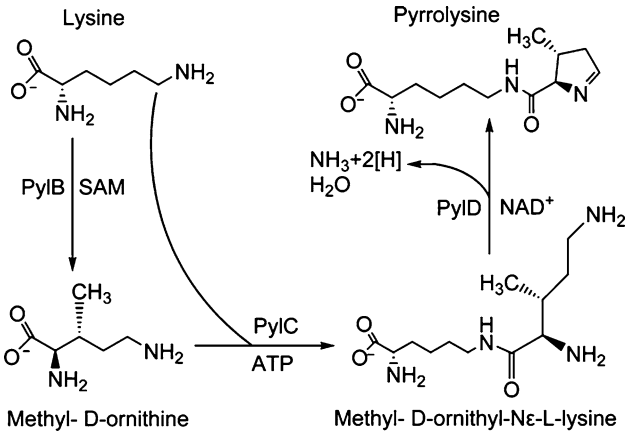

Scheme 1 Biosynthesis pathway of pyrrolysine

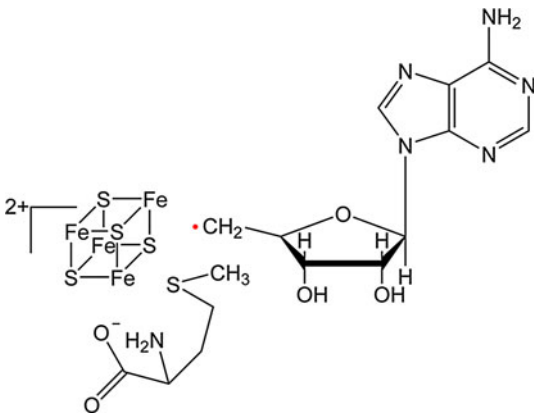

Fig. 1 Structure of $[4Fe–4S]^{2+}$ cluster, methionine, and 5′-deoxyadenosyl radical

It should be noted that parts of the pathway in Scheme 1 and the proposed mechanism in Scheme 2 are only based on indirect experimental data, and the methylornithine has not been directly isolated yet [9, 10]. Recently, the structure of pylB in complex with methylornithine has been determined by X-ray crystallography [9]. The active-site cavity of pylB contains an iron–sulfur cluster, SAM, and methylornithine, which implies that methylornithine has been generated by pylB catalysis. By examining the structure of methylornithine in the active site of enzyme, it was found that the stereochemistry of methylornithine was 2R,3R, further justifying the proposed mechanism. However, to our knowledge, theoretical study on the reaction mechanism of pylB is still lacking. In particular, which reaction step is rate limiting and how the lysine-derived radical undergoes a skeletal rearrangement are still unclear.

In this paper, the reaction mechanism of pylB has been studied by using quantum mechanical/molecular mechanical (QM/MM) approach, which is a popular tool for studying enzymatic reactions [20–23]. The detailed energetic profile of the overall reaction and the structures of all intermediates and transition states along the reaction pathway are presented. To our knowledge, this is the first computational study of the reaction mechanism of pylB.

2 Methods

2.1 Computational model

The initial structure was based on the crystal structure of methylornithine synthase (pylB) in complex with iron–sulfur, SAM, and methylornithine from Protein Data Bank (PDB code: 3T7 V) [9]. To obtain a reasonable structure of methylornithine synthase in complex with the substrate

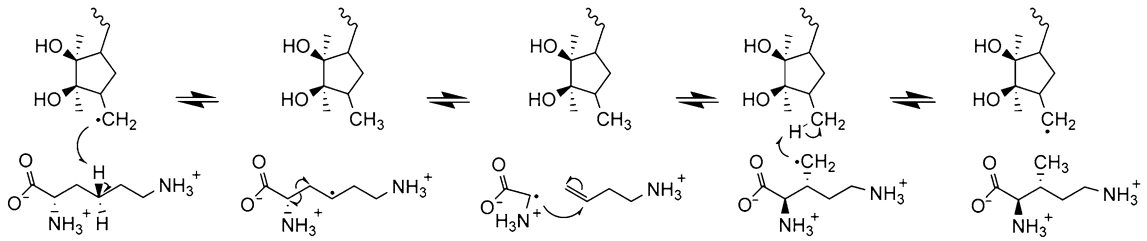

Scheme 2 Hypothetical reaction mechanism for PylB

(lysine), the methylornithine was firstly removed from the active site, and then, an L-lysine was docked into the active site by AutoDockTools 4.0 [24]. Based on a grid module, the grid scale was set as 60 × 60 × 60 Å with the spacing of 0.375 Å between the grid points. During the docking, the protein was kept rigid, while all the torsional bonds of lysine were kept free in 50 independent runs. The docking results were clustered based on a 2.0 Å criterion of root-mean-square deviation (RMSD). Actually, only one cluster was obtained, i.e., the 50 poses have very similar conformation and protein–ligand interaction energies. Thus, one typical conformation was chosen for the following simulation. Based on the experimental condition, the protonation states of all titratable residues were checked with pKa prediction program, PROPKA3.1 at PH 8.0 [25–28]. According our calculations, two amine groups of lysine were protonated, while all other titratable residues adopt their normal protonation states. Since the reaction is initiated by an electron transfer from $[4Fe–4S]^{+}$ cluster to sulfonium motif of SAM to generate a $[4Fe–4S]^{2+}$ cluster, a methionine and a 5′-deoxyadenosyl radical are the actual catalytic transponder [17]. Their structures are shown in Fig. 1. Besides, the missing hydrogen atoms were added to the system with the HBUILD program in the CHARMM package [29]. The system was fully solvated in a sphere of TIP3P [30] water molecules with a radius of 37.15 Å and was neutralized using 4 sodium cations at random positions. Finally, the resulting system contains 5,486 atoms of protein–substrate complex, 14,313 atoms of TIP3P water, and 4 atoms of sodium cations. After a series of minimizations, 10 ns MD simulation was performed with the CHARMM22/CMAP force field [29, 31, 32] to equilibrate the system, and the last snapshot was selected as the starting structure for the QM/MM optimizations. During all minimizations and MD simulations, iron–sulfur cluster, SAM, and lysine were kept frozen. For comparison, the MD simulations with lysine kept free were also performed. Lysine was still stable at the active site. The typical conformation was shown in the supplementary materials (Figure S1).

2.2 QM/MM calculations

The reaction mechanism of methylornithine synthase was investigated by using QM/MM calculations [33, 34], in which the interfaces of QM and MM regions are linked by hydrogen atoms [35]. The side chain of Asp279, lysine, and part of Ado radical were included in the QM region, which contains 49 atoms plus two hydrogen link atoms, as shown in Fig. 2. The rest of the system was included in the MM region. In the QM/MM calculations, only atoms within 20 Å of lysine substrate of MM region and QM region were allowed to move, the remaining atoms of the system were frozen. For the system, the total charge of QM region is 0 and the spin multiplicity is 2. The QM region was treated with DFT with B3LYP functional [36–39], which has been proved to be successful in a number of different studies on radical-containing enzymes [40, 41]. MM region was treated by molecular mechanics with the CHARMM22 force field [32]. For the QM region, the geometry optimizations were performed at the B3LYP/6-31G(d,p) level, whereas the spin density and single-point calculations were performed using a basis set of 6-311++G(d,p). All QM/MM calculations were done by ChemShell package [42] combining Turbomole [43] (QM region) and DL-POLY [44] (MM region) programs. Hybrid delocalized internal coordinates (HDLC) optimizer [45] in ChemShell were performed for geometry optimizations. Minima were searched by a quasi-Newton limited memory Broyden-Fletcher-Goldfarb-Shanno (L-BFGS) method. Scans over bond length and dihedral angle were performed. To find transition states, the highest point of the potential energy profile along the reaction coordinate was optimized by the partitioned rational function optimization (P-RFO) algorithm.

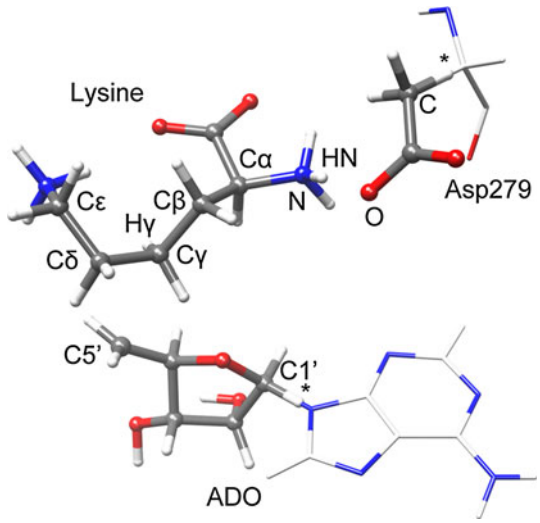

Fig. 2 The QM region (ball-and-stick) including part of Ado, lysine, and side chain of Asp 279. The interface between the QM and MM regions is linked by hydrogen link atoms (indicated by *asterisks*). Carbon is shown in *gray*, oxygen in *red*, hydrogen in *white*, and nitrogen in *blue*

3 Results and discussion

3.1 Structure of the PylB–lysine complex

To obtain a reasonable structure of methylornithine synthase in complex with a lysine, an L-lysine was docked into the active site of methylornithine synthase. Figure 3 shows

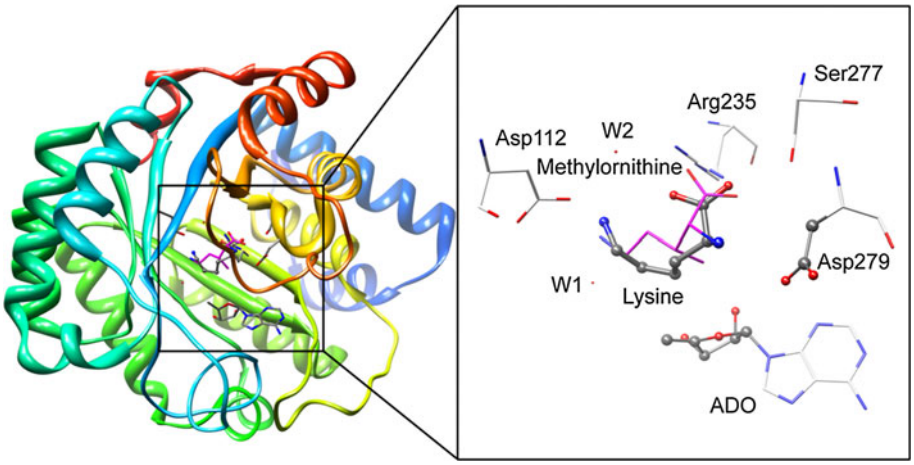

Fig. 3 Crystal structure of methylornithine synthase in complex with (2R,3 R)-3-methylornithine. For comparison, the docking structure of lysine is also shown in the same image. Lysine is shown as a *dim gray* skeleton (2R,3R)-3-methylornithine is shown as a *magenta* skeleton

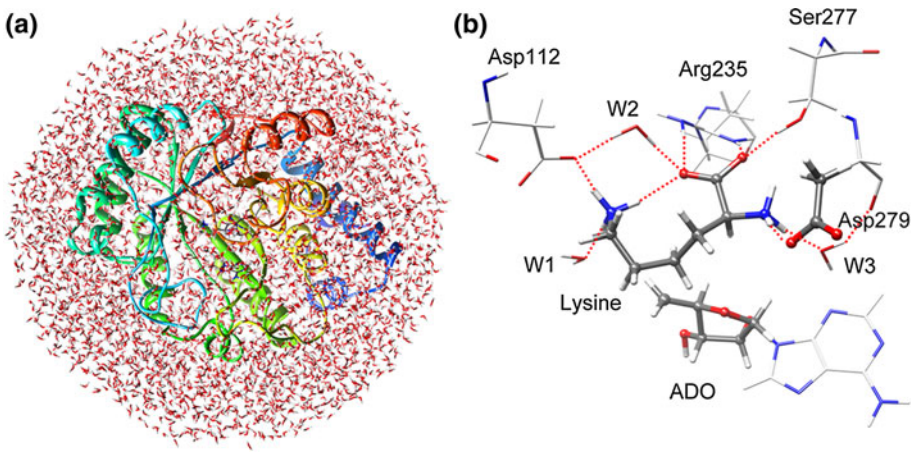

Fig. 4 Optimized structures of solvated model (**a**) and active site (**b**)

the comparison of docking result and crystal structure of methylornithine synthase complexed with (2R,3R)-3-methylornithine. One can see that the positions of two amino groups and carboxyl group of lysine are close to (2R,3R)-3-methylornithine, implying the docking result is reasonable and suitable for studying the reaction mechanism.

The optimized structure of methylornithine synthase and its active site is shown in Fig. 4. Lysine is stabilized by forming a network of hydrogen bonds with the side chains of Asp112, Arg235, Ser277, Asp279, and three water molecules. Besides, three water-mediated hydrogen bonds are formed. A hydrogen atom bonded to the lysine Cγ is situated in the vicinity of Ado radical, facilitating its abstraction by Ado radical.

3.2 Calculated reaction mechanism

From our calculations, we found that the conversion of lysine to (2R,3R)-3-methylornithine proceeds in seven elementary steps, which is similar with the proposed mechanism as shown in Scheme 2: (1) Ado radical abstracts a hydrogen atom from the position Cγ methylene of lysine to generate a lysine-derived radical; (2) the protonated α-amino group of lysine denotes its proton to Asp279; (3) Cα–Cβ bond of lysine radical undergoes a hemolytic cleavage to form a glycyl radical and aminobutene; (4) aminobutene rotates along the C–C single bond (original Cγ–Cδ bond in lysine); (5) glycyl radical rebinds to the C=C double bond of aminobutene; (6) the protonated Asp279 returns the proton back to the α-amino group of methylornithine; (7) the methylene radical of methylornithine abstracts a hydrogen atom from Ado to complete the catalytic reaction.

Our calculations started with the abstraction of a hydrogen atom from lysine by the Ado radical to generate the lysine-derived radical. All the optimized structures of reactant, transition states, and intermediates of the QM region are shown in Fig. 5. According to the our results, the conversion of lysine to (2R,3R)-3-methylornithine follows a fragmentation–recombination mechanism.

As can been seen from Fig. 5, the Ado radical firstly abstracts a hydrogen from the Cγ methylene group of lysine (R) via a transition state (TS1) to generate a lysine-derived radical intermediate (IM1). In TS1, the distance between C5′ carbon of the ribose moiety and the hydrogen

at Cγ methylene group of lysine is shortened from 2.78 to 1.41 Å. Meanwhile, the distance between that hydrogen and Cγ carbon of lysine increases from 1.10 to 1.36 Å. On the basis of our calculation, the energy barrier of this step is 20.4 kcal/mol, which is shown in Fig. 6. In IM1, the distance between C5′ carbon and the hydrogen atom further decreases to 1.09 Å. In reactant R, the initial radical is primarily localized at the C5′ carbon of the ribose moiety [40]. After the hydrogen atom transfers to the Ado moiety, the radical is mainly localized at the Cγ carbon of lysine.

The second step corresponds to a proton transfer from the α-amino group of lysine to the carboxyl group of Asp 279, and the energy barrier of this step is only 2.5 kcal/mol. It should be noted that the relative energy of IM2 is only 0.2 kcal/mol lower than TS2 at B3LYP/6-31G(d,p) level. Further single-point calculations at the level of B3LYP/6-311++G(d,p) indicate that the relative energy of IM2 is even higher than TS2 by 0.5 kcal/mol, implying the unstable characteristic of IM2, which can easily change back to IM1. This may be caused by the relatively small QM region. We noted that the position of the frontier atom (the QM carbon at the border) of Asp279 is situated in the vicinity of the reactive center. Along the reaction path, the Mulliken charges of heavy frontier atoms should remain nearly constant. But in our calculations, the Mulliken charge of the heavy frontier atom of Asp279 changes from −0.38 in IM1 to −0.40 in IM2 (shown in Table S1 in supplementary materials), which may influences the relative energies of the species.

In the next step, IM2 undergoes a hemolytic cleavage of Cα–Cβ bond of lysine to generate the glycyl radical and aminobutene (IM3). The energy barrier of cleavage of the

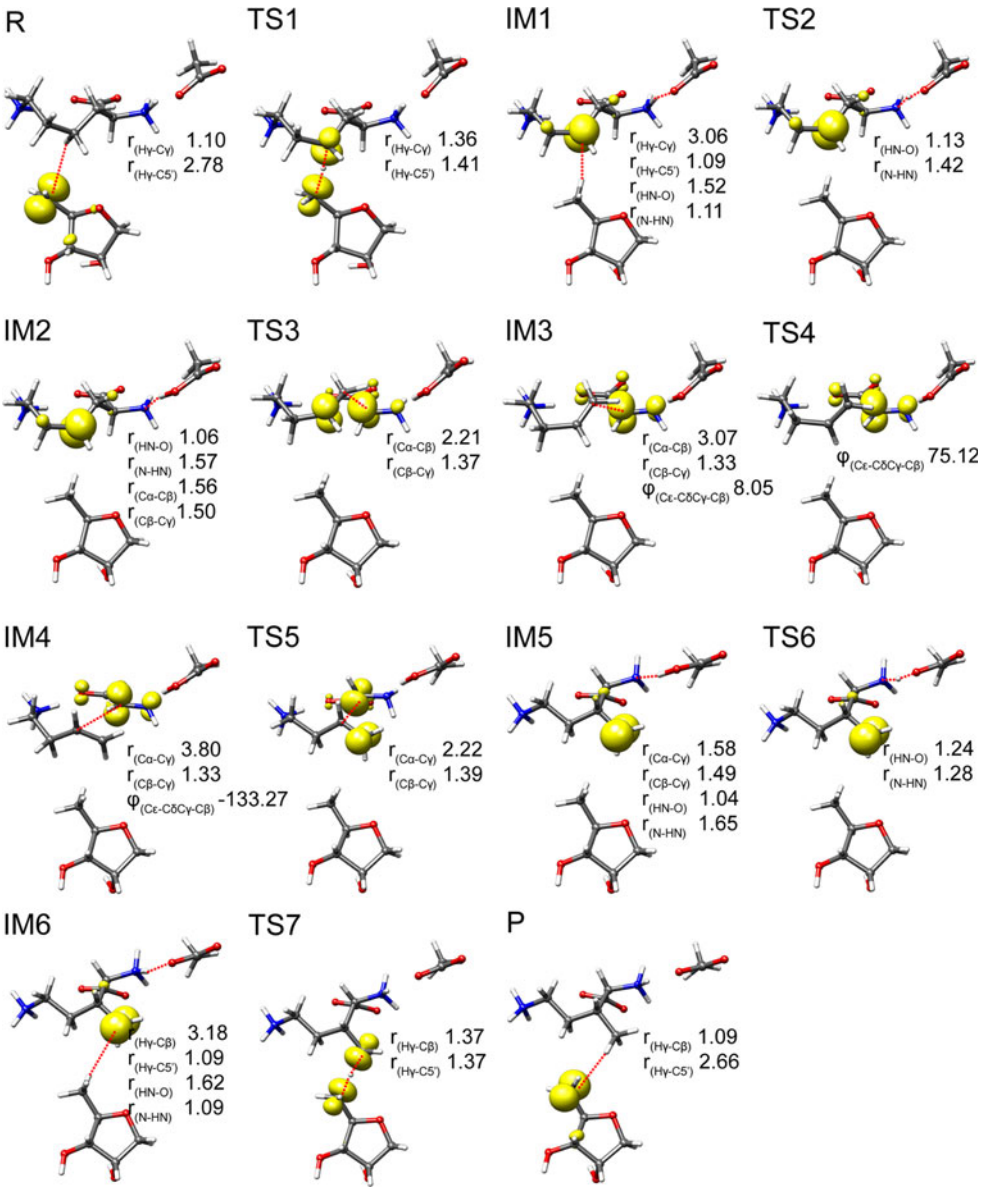

Fig. 5 Optimized structures of the reactant, transition states, and product. Distances are given in Å; dihedral angles of carbon backbone (Cε-Cδ-Cγ-Cβ) of aminobutene in IM3, TS4, and IM4 are in degree. The 3D spin density is shown in *orange ball* (the isovalue of 0.01 au)

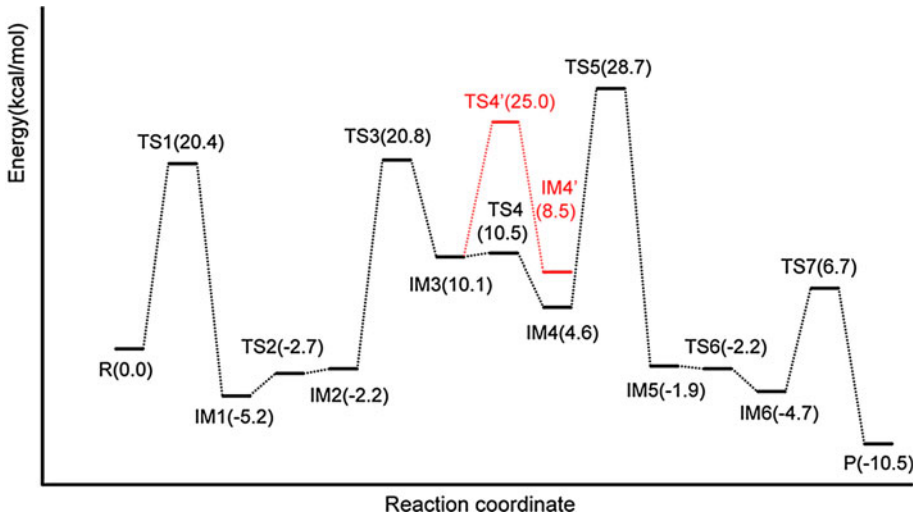

Fig. 6 Energy profiles for lysine mutase reaction

Cα–Cβ bond is 23.0 kcal/mol, which is a little higher than that of the first step. In IM3, the radical is mainly localized at the Cα carbon of glycyl molecule.

Subsequently, the skeleton of aminobutene undergoes an intramolecular rotation along Cγ–Cδ bond, in which the dihedral angle of carbon backbone (Cε–Cδ–Cγ–Cβ) changes from 8.05° (in IM3) to −133.27° (IM4) with an energy barrier of only 0.4 kcal/mol.

The next step is the ligation of glycyl radical to aminobutene leading to the formation of IM5. In IM5, the newly formed Cα–Cγ bond distance changes from 3.80 Å in IM4 to 1.58 Å via 2.22 Å in TS5. Meanwhile, the double bond of Cβ–Cγ changes to single bond with its distance increases from 1.33 to 1.49 Å. The energy barrier of this ligation step is calculated to be 24.1 kcal/mol. In IM5, the radical is primarily localized at the methylene group.

The aminobutene may reunite directly with the glycyl radical without undergoing the above intramolecular rotation. The calculated structures of transition state (TS4′) and intermediate (IM4′) are shown in Fig. 7. One can see that the distances of Cα–Cγ in TS4′ and IM4′ are 2.17 and 1.59 Å, respectively, which are almost identical to those in TS5 and IM5, but their conformations are completely different. The stereochemistry of IM4′ is 2S,3S, while that of IM5 is 2R,3R. We note that the direct ligation of glycyl radical to aminobutene corresponds to a small barrier (14.9 kcal/mol), as shown in Fig. 6. But in IM4′, the distance between the Cβ and the hydrogen to be transferred reaches to a length of 5.36 Å, which is difficult for the following reaction.

In the last two steps, the proton on the carboxyl of Asp 279 transfers back firstly to the α-amino group of the substrate, and then, the methylene radical abstracts a hydrogen from Ado leading to the formation of (2R,3R)-3-methylornithine product and regeneration of the Ado radical. The relative energy of TS6 is 0.9 kcal/mol higher

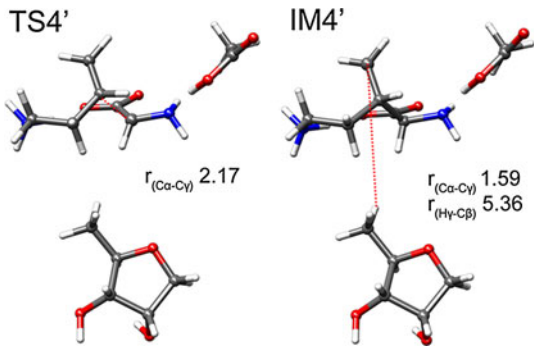

Fig. 7 Optimized structures of TS4′ and IM4′. Distances are given in Å

than IM5 at B3LYP/6-31G(d,p) level. After single-point calculations at the level of B3LYP/6-311++G(d,p), the relative energy of TS6 is −0.3 kcal/mol lower than IM5. Similar to the second step, this may be caused by the small QM model. The energy barrier of the last step is 11.4 kcal/mol.

In general, three steps correspond to the larger energy barriers. One is the initial abstraction of hydrogen atom from the lysine by Ado radical, corresponding to an energy barrier of 20.4 kcal/mol. The other two steps relate to the hemolytic cleavage of Cα–Cβ bond of lysine and the ligation of glycyl radical with aminobutene, with the energy barriers of 23.0 and 24.1 kcal/mol, respectively, which are most possible rate-limiting steps.

4 Conclusions

In this work, the mechanism of lysine mutase reaction has been studied by using the QM/MM approach. The calculation results indicate that the conversion of L-lysine to (2R,3R)-3-methylornithine follows a fragmentation–recombination mechanism through seven elementary steps.

The hemolytic cleavage of Cα–Cβ bond of lysine and the ligation of glycyl radical with aminobutene corresponds to the energy barriers of 23.0 and 24.1 kcal/mol, respectively, both of which are possible rate limiting. It is the intramolecular rotation of intermediate aminobutene that controls the stereochemistry of the catalytic reaction. Asp 279 functions as general acid/base in the reaction. The other pocket residues such as Asp112, Arg235, and Ser277 form a network of hydrogen bonds responsible for orientation of the substrate. This study sheds light on the atomistic details of the reaction mechanism and helps to understand how the methylornithine synthase (PylB) catalyzes the carbon skeleton rearrangement of lysine.

Acknowledgments This work was supported by the Natural Science Foundation of China (21173129, 31200048).

References

1. Srinivasan G, James CM, Krzycki JA (2002) Pyrrolysine encoded by UAG in Archaea: charging of a UAG-decoding specialized tRNA. Science 296:1459–1462
2. Hao B, Gong W, Ferguson TK, James CM, Krzycki JA, Chan MK (2002) A new UAG-encoded residue in the structure of a methanogen methyltransferase. Science 296:1462–1466
3. Atkins JF, Gesteland R (2002) The 22nd amino acid. Science 296:1409–1410
4. Blight SK, Larue RC, Mahapatra A, Longstaff DG, Chang E, Zhao G, Kang PT, Green-Church KB, Chan MK, Krzycki JA (2004) Direct charging of $tRNA_{CUA}$ with pyrrolysine in vitro and in vivo. Nature 431:333–335
5. Ibba M, Söll D (2002) Genetic code: introducing pyrrolysine. Curr Biol 12:R464–R466
6. Krzycki JA (2004) Function of genetically encoded pyrrolysine in corrinoid-dependent methylamine methyltransferases. Curr Opin Chem Biol 8:484–491
7. Mahapatra A, Patel A, Soares JA, Larue RC, Zhang JK, Metcalf WW, Krzycki JA (2006) Characterization of a methanosarcina acetivorans mutant unable to translate UAG as pyrrolysine. Mol Microbiol 59:56–66
8. Gaston MA, Jiang RS, Krzycki JA (2011) Functional context, biosynthesis, and genetic encoding of pyrrolysine. Curr Opin Microbiol 14:342–349
9. Quitterer F, List A, Eisenreich W, Bacher A, Groll M (2012) Crystal structure of methylornithine synthase (PylB): insights into the pyrrolysine biosynthesis. Angew Chem Int Ed 51:1339–1342
10. Gaston MA, Zhang LW, Green-Church KB, Krzycki JA (2011) The complete biosynthesis of the genetically encoded amino acid pyrrolysine from lysine. Nature 471:647–650
11. Wang SC, Frey PA (2007) S-adenosylmethionine as an oxidant: the radical SAM superfamily. Trends Biochem Sci 32:101–110
12. Rother M, Krzycki JA (2010) Selenocysteine, pyrrolysine, and the unique energy metabolism of methanogenic archaea. Archaea 2010:453642
13. Buckel W, Golding BT (1996) Glutamate and 2-methyleneglutarate mutase: from microbial curiosities to paradigms for coenzyme B_{12}-dependent enzymes. Chem Soc Rev 25:329–337
14. Marsh ENG, Ballou DP (1998) Coupling of cobalt-carbon bond homolysis and hydrogen atom abstraction in adenosylcobalamin-dependent glutamate mutase. Biochemistry 37:11864–11872
15. Chih HW, Marsh ENG (1999) Pre-steady-state kinetic investigation of intermediates in the reaction catalyzed by adenosylcobalamin-dependent glutamate mutase. Biochemistry 38:13684–13691
16. Rommel JB, Kästner J (2011) The fragmentation-recombination mechanism of the enzyme glutamate mutase studied by QM/MM simulations. J Am Chem Soc 133:10195–10203
17. Kamachi T, Kouno T, Doitomi K, Yoshizawa K (2011) Generation of adenosyl radical from S-adenosylmethionine (SAM) in biotin synthase. J Inorg Biochem 105:850–857
18. Dowling DP, Vey JL, Croft AK, Drennan CL (2012) Structural diversity in the AdoMet radical enzyme superfamily. Biochim Biophys Acta 1824:1178–1195
19. Fontecave M, Mulliez E, Ollagnier-de-Choudens S (2001) Adenosylmethionine as a source of 5′-deoxyadenosyl radicals. Curr Opin Chem Biol 5:506–511
20. Grigorenko BL, Shadrina MS, Topol IA, Collins JR, Nemukhin AV (2008) Mechanism of the chemical step for the guanosine triphosphate (GTP) hydrolysis catalyzed by elongation factor Tu. Biochim Biophys Acta 1784:1908–1917
21. Lin H, Truhlar DG (2007) QM/MM: what have we learned, where are we, and where do we go from here? Theor Chem Acc 117:185–199
22. Friesner RA, Guallar V (2005) Ab initio quantum chemical and mixed quantum mechanics/molecular mechanics (QM/MM) methods for studying enzymatic catalysis. Annu Rev Phys Chem 56:389–427
23. Hou QQ, Gao J, Liu YJ, Liu CB (2012) A QM/MM study on the catalytic mechanism of pyruvate decarboxylase. Theor Chem Acc 131:1280
24. Morris GM, Goodsell DS, Halliday RS, Huey R, Hart WE, Belew RK, Olson AJ (1998) Automated docking using a Lamarckian genetic algorithm and an empirical binding free energy function. J Comput Chem 19:1639–1662
25. Li H, Robertson AD, Jensen JH (2005) Very fast empirical prediction and rationalization of protein pKa values. Proteins: Struct, Funct, Bioinf 61:704–721
26. Bas DC, Rogers DM, Jensen JH (2008) Very fast prediction and rationalization of pKa values for protein-ligand complexes. Proteins: Struct, Funct, Bioinf 73:765–783
27. Olsson MHM, Søndergard CR, Rostkowski M, Jensen JH (2011) PROPKA3: consistent treatment of internal and surface residues in empirical pKa predictions. J Chem Theory Comput 7:525–537
28. Søndergaard CR, Olsson MHM, Rostkowski M, Jensen JH (2011) Improved treatment of ligands and coupling effects in empirical calculation and rationalization of pKa values. J Chem Theory Comput 7:2284–2295
29. Brooks BR, Bruccoleri RE, Olafson BD, States DJ, Swaminathan S, Karplus M (1983) CHARMM: a program for macromolecular energy, minimization, and dynamics calculations. J Comput Chem 4:187–217
30. Jorgensen WL, Chandrasekhar J, Madura JD, Impey RW, Klein ML (1983) Comparison of simple potential functions for simulating liquid water. J Chem Phys 79:926–935
31. Chen J, Im W, Brooks CL (2006) Balancing solvation and intramolecular interactions: toward a consistent generalized born force field. J Am Chem Soc 128:3728–3736
32. MacKerell AD Jr, Bashford D, Bellott M, Dunbrack RL Jr, Evanseck JD, Field MJ, Fischer S, Gao J, Guo H, Ha S, Joseph-McCarthy D, Kuchnir L, Kuczera K, Lau FTK, Mattos C, Michnick S, Ngo T, Nguyen DT, Prodhom B, Reiher WE III, Roux B, Schlenkrich M, Smith JC, Stote R, Straub J, Watanabe M, Wiorkiewicz-Kuczera J, Yin D, Karplus M (1998) All-atom empirical potential for molecular modeling and dynamics studies of proteins. J Phys Chem B 102:3586–3616

33. Warshel A, Karplus M (1972) Calculation of ground and excited state potential surfaces of conjugated molecules. I. formulation and parametrization. J Am Chem Soc 94:5612–5625
34. Warshel A, Levitt M (1976) Theoretical studies of enzymic reactions: dielectric, electrostatic and steric stabilization of the carbonium ion in the reaction of lysozyme. J Mol Biol 103: 227–249
35. Field MJ, Bash PA, Karplus M (1990) A combined quantum mechanical and molecular mechanical potential for molecular dynamics simulations. J Comput Chem 11:700–733
36. Vosko SH, Wilk L, Nusair M (1980) Accurate spin-dependent electron liquid correlation energies for local spin density calculations: a critical analysis. Can J Phys 58:1200–1211
37. Lee C, Yang W, Parr RG (1988) Development of the Colle-Salvetti correlation-energy formula into a functional of the electron density. Phys Rev B 37:785–789
38. Becke AD (1993) Density-functional thermochemistry. III. The role of exact exchange. J Chem Phys 98:5648–5652
39. Stephens PJ, Devlin FJ, Chabalowski CF, Frisch MJ (1994) Ab initio calculation of vibrational absorption and circular dichroism spectra using density functional force fields. J Phys Chem 98:11623–11627
40. Feliks M, Ullmann GM (2012) Glycerol dehydratation by the B_{12}-independent enzyme may not involve the migration of a hydroxyl group: a computational study. J Phys Chem B 116: 7076–7087
41. Himo F, Siegbahn PEM (2003) Quantum chemical studies of radical-containing enzymes. Chem Rev 103:2421–2456
42. Sherwood P, de Vries AH, Guest MF, Schreckenbach G, Catlow CRA, French SA, Sokol AA, Bromley ST, Thiel W, Turner AJ, Billeter S, Terstegen F, Thiel S, Kendrick J, Rogers SC, Casci J, Watson M, King F, Karlsen E, Sjøvoll M, Fahmi A, Schäfer A, Lennartz C (2003) QUASI: a general purpose implementation of the QM/MM approach and its application to problems in catalysis. J Mol Struct (Theochem) 632:1–28
43. Ahlrichs R, Bär M, Häser M, Horn H, Kölmel C (1989) Electronic structure calculations on workstation computers: the program system turbomole. Chem Phys Lett 162:165–169
44. Smith W, Forester TR (1996) DL_POLY_2.0: a general-purpose parallel molecular dynamics simulation package. J Mol Graph 14:136–141
45. Billeter SR, Turner AJ, Thiel W (2000) Linear scaling geometry optimisation and transition state search in hybrid delocalised internal coordinates. Phys Chem Chem Phys 2:2177–2186